

Hierarchical Proliferation of Higher-Rank Symmetry Defects in Fractonic Superfluids

Jian-Keng Yuan,¹ Shuai A. Chen,^{2,*} and Peng Ye^{1,†}

¹*School of Physics, State Key Laboratory of Optoelectronic Materials and Technologies, and Guangdong Provincial Key Laboratory of Magnetoelectric Physics and Devices, Sun Yat-sen University, Guangzhou, 510275, China*

²*Department of Physics, The Hong Kong University of Science and Technology, Hong Kong SAR, China*

(Dated: Tuesday 6th December, 2022)

Symmetry defects, e.g., vortices in conventional superfluids, play a critical role in a complete description of symmetry-breaking phases. In this paper, we develop the theory of symmetry defects in fractonic superfluids, i.e., spontaneously higher-rank symmetry (HRS) breaking phases. By Noether's theorem, HRS is associated with the conservation law of higher moments, e.g. dipoles, quadrupoles, and angular moments. We establish finite-temperature phase diagrams by identifying a series of topological phase transitions via the renormalization group flow equations and Debye-Hückel approximation. Accordingly, a series of Kosterlitz-Thouless topological transitions are found to occur successively at different temperatures, which are triggered by proliferation of defects, defect bound states, and so on. Such a *hierarchical proliferation* brings rich phase structures. Meanwhile, a screening effect from sufficiently high density of defect bound states leads to instability and collapse of the intermediate temperature phases, which further enriches the phase diagrams. For concreteness, we consider a fractonic superfluid in which "angular moments" are conserved. We then present the general theory, in which other types of HRS can be analyzed in a similar manner. Further directions are present at the end of the paper.

I. INTRODUCTION

The concept of symmetry and its spontaneous breaking has influenced quantum physics, from phases and phase transitions to the Standard Model of fundamental forces. A symmetry breaking phase can be characterized by an order parameter that varies with respect to symmetry operation and fluctuates in the vicinity of mean-field configurations. Distinct from smooth fluctuations, such as phonons and rotons, a singularity can be induced by symmetry defects, which tends to disorder the phase and restore symmetry. In a conventional 2D superfluid where $U(1)$ global symmetry related to particle number conservation gets spontaneously broken, for example, the symmetry defects "superfluid vortex" at sufficiently low temperatures are confined into dipole-like bound states such that the superfluid phase is sustained against thermal fluctuations. At a critical value T_c , vortices begin to be released from bound states, which eventually results in a vortex proliferation that destroys the superfluid phase and restores symmetry at temperatures higher than T_c . This is one of great achievements that lead to 2016 Nobel Prize in Physics, namely, celebrated Kosterlitz-Thouless (KT) physics [1–3], which provides one of most influential prototypes of topological phase transitions driven by symmetry defects.

As symmetry is an indispensable ingredient in the above KT physics, the goal of this paper is to explore KT-like physics in many-body systems where *higher-rank symmetry* (HRS) gets spontaneously broken. Let us first give a brief introduction to HRS. Electromagnetism textbook tells us, by starting with the particle density ρ , we can express a series of multipole moments, such as $\rho x^a, \rho x^a x^b, \dots$. While the conservation of charge, i.e., the integration of ρ over the whole space, is a very familiar fact in, e.g., metals and insulators,

it is also meaningful for considering systems with conserved higher moments. Furthermore, Noether's theorem indicates that each of conserved quantities here must be associated with an underlying continuous symmetry, which is nothing but aforementioned HRS. In the literature, the condensed matter physics of such type of symmetry has been initiated and paid great attentions to in the field of fracton physics [4, 5] where diverse quantum phenomena have been discovered, including system-size dependent noise-immune ground state degeneracy, exotic quantum dynamics, see, e.g., Refs. [6–20]. As a side, while there are alternative terminologies in the literature, here we call these symmetries "higher rank symmetry" due to the resultant higher-rank tensor gauge field after gauging it.

By noting that there have been great triumphs in the conventional spontaneously symmetry-breaking phase, we are motivated to ask if there is novel many-body physics by instead considering HRS. For example, in the framework of HRS, what can we expect for the superfluid-like phase, off-diagonal long-range order, Mermin-Wagner-like theorem, symmetry defects, and KT-like physics? Along this line of thinking, Refs. [21–24] construct concrete minimal models for realizing unconventional ordered phases dubbed *fractonic superfluids*, in which higher-rank $U(1)$ symmetry gets spontaneously broken in various fashions. Many exotic phenomena beyond the conventional symmetry-breaking phases have been identified in various channels [21–27]. In this paper, we will focus on HRS defects and HRS-generalization of KT physics in fractonic superfluids.

In this paper, we establish a general framework of finite-temperature phase diagrams and a series of KT topological phase transitions driven by proliferation of either HRS symmetry defects or defect bound states. We discover that, thermally activated HRS defects generally constitute a hierarchy of bound states, such as dipole with neutral charge [**Terminology clarification:** *Hereafter, unless otherwise specified, charge means the vorticity/winding number of HRS defect, while dipole, quadrupole, etc. really are formed by defects rather than original condensed bosons.*],

* chsh@ust.hk

† yepeng5@mail.sysu.edu.cn

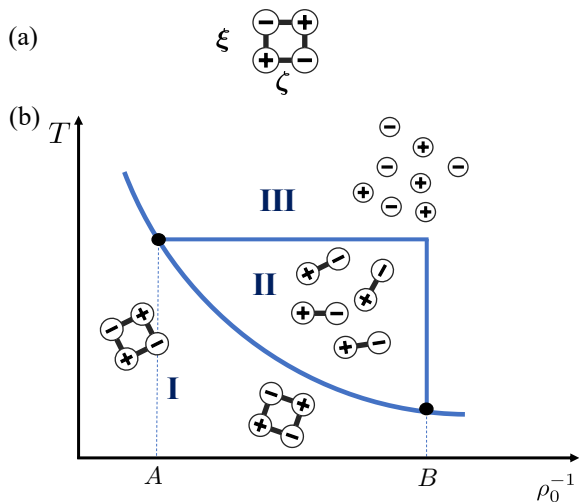


FIG. 1. Global phase diagram. (a) A quadrupole bound state of a pair of a unit defect and a unit anti-defect. (b) Finite-temperature phase diagram from the renormalization group analysis and Debye-Hückel approximation. T and ρ_0^{-1} are respectively temperature and superfluid stiffness inverse. In Phase-I, defects Θ are confined in the form of quadrupole bound states. In Phase-II, defects are confined in the form of dipole bound states. In Phase-III, defects are fully released from bound states and are wildly mobile. The locations of A and B depend on core energy values of both defects and dipole bound states (see the main text). Two topological transitions occur successively from Phase-I, Phase-II, to Phase-III. A direct transition from Phase-I to Phase-III occurs if ρ_0^{-1} is outside the domain (A, B) .

quadrupole [Fig. 1(a)] with both neutral charge and dipole moment, and so on. They bear a series of self-energy divergence, e.g., $\ln L, L, L^2, \dots$, with L being the system size. Upon increasing temperature, various bound states successively get dissolved, from which new bound states of defects are successively released and then proliferate. After a series of KT transitions, HRS defects are finally released from all bound states and become mobile at high temperatures.

We take the conservation of so-called *angular moments* as a concrete example [22, 23] and then go to general theory. Through renormalization-group (RG) analysis and Debye-Hückel approximation, we identify two characteristic KT transitions and three distinct phases as shown in Fig. 1(b). In Phase-I, defects are confined into quadrupole bound states such that superfluidity is sustained. If further increasing temperature with ρ_0^{-1} being in the domain (A, B) , Phase-I is transitioned into Phase-II at T_{c1} , which is the critical temperature of the first KT transition where quadrupole bound states get dissolved and dipole bound states get proliferated. In Phase-II, superfluidity is destroyed. Then, if temperature is further increased, dipole bound states form a plasma with high density which drastically renormalizes the bare interaction between defects. As a result, the second KT transition occurs at T_{c2} , which sends the system into Phase-III. As the defects are no more bound in the form of BS, defects are wildly mobile in Phase-III, which is similar to the episode in the movie *Pirates of the Caribbean*: the enraged goddess Calypso, once

being released from human form, generates a massive maelstrom. On the other hand, if ρ_0^{-1} is either too small or too large, Phase-I is directly transitioned to Phase-III in Fig. 1.

The remainder of this paper is organized as follows. In Sec. II, we concretely set up the minimal model, higher-rank symmetry, and defect configurations. In Sec. III, we study Phase-I where defects are confined in quadrupole-like bound states. In Sec. IV, we study Phase-II where defects are confined in dipole-like bound states. Key results are summarized in Sec. IV A. In Sec. V, we study Phase-III where defects are deconfined. Key results are summarized in Sec. V A. In Sec. VI, we generalize the above study to more complex higher-rank symmetry. In The paper is concluded in Sec. VII.

II. MINIMAL MODEL, HIGHER-RANK SYMMETRY, AND DEFECT CONFIGURATIONS

We start with the following minimal Hamiltonian that conserves angular moments [22–24],

$$H = |\partial_1 \hat{\Phi}_1|^2 + |\partial_2 \hat{\Phi}_2|^2 + \hat{V}_0 + \hat{V}_1, \quad (1)$$

where

$$\hat{V}_0 = \sum_{\alpha=1}^2 -\mu \hat{\rho}_\alpha + \frac{g}{2} \hat{\rho}_\alpha^2 \quad (2)$$

and

$$\hat{\rho}_\alpha = \hat{\Phi}_\alpha^\dagger \hat{\Phi}_\alpha. \quad (3)$$

Here $\hat{\Phi}_{1,2}$ denote two components of complex bosonic fields. \hat{V}_0 includes a repulsive interaction and a chemical potential term. The term

$$\hat{V}_1 = K |\hat{\Phi}_1 \partial_1 \hat{\Phi}_2 + \hat{\Phi}_2 \partial_2 \hat{\Phi}_1|^2 \quad (4)$$

represents a two-particle correlated hopping process. Apart from the particle number conservation for each component, the model has an extra $U(1)$ to conserve the total *angular moments* that are a vectorial generalization of dipoles:

$$Q_{12} = \int d^2 \mathbf{r} (\hat{\rho}_1 y - \hat{\rho}_2 x), \quad (5)$$

where $\mathbf{r} = (x, y)$. Indeed, one may check that

$$[Q_{12}, H] = 0 \quad (6)$$

upon applying canonical quantization and regarding Q_{12} as a generator of HRS. Thus, a group element of HRS can be expressed as $e^{i\theta Q_{12}}$. Here we discard symmetry-respecting terms with more complicated momentum dependence as all these terms are irrelevant at low energies. Once \hat{V}_0 forms a Mexican hat, we obtain a *fractonic superfluid* phase with off-diagonal long-range order and non-vanishing order parameters $\langle \hat{\Phi}_1 \rangle = \langle \hat{\Phi}_2 \rangle \neq 0$ whose low-energy effective Hamiltonian reads

$$H[\theta_1, \theta_2] = \frac{1}{2} \rho_0 [(\partial_1 \theta_1)^2 + (\partial_2 \theta_2)^2 + (\partial_1 \theta_2 + \partial_2 \theta_1)^2], \quad (7)$$

where $\theta_{1,2}$ are Goldstone modes. Without loss of generality, we set $K\rho_0 = 1$ with ρ_0 being the superfluid stiffness, which simplifies the formulas. As the velocity fields $v_{\alpha\beta}$ [24] ($\alpha, \beta = 1, 2$) of α th component bosons of β th direction in fractonic superfluids are

$$v_{\alpha\beta} = \delta_{\alpha\beta}\partial_\alpha\theta_\alpha + (1 - \delta_{\alpha\beta})(\partial_\alpha\theta_\beta + \partial_\beta\theta_\alpha), \quad (8)$$

the Hamiltonian in Eq. (7) reduces to the following compact form

$$H = \frac{\rho_0}{2} \int d^2\mathbf{r} \sum_{\alpha\beta} v_{\alpha\beta}^2. \quad (9)$$

The bare superfluid stiffness ρ_0 , a hallmark of the superfluid phase, can be reduced by thermal defects. In general, due to thermally activated topological defects, we can decompose the fields θ_α into a smooth part $\tilde{\theta}_\alpha$ and singular part θ_α^s , i.e. $\theta_\alpha = \tilde{\theta}_\alpha + \theta_\alpha^s$. And the velocity field follows a similar decomposition, the smooth part $\tilde{v}_{\alpha\beta}$ describing the superfluidity and the singularity part $v_{s,\alpha\beta}$ describing topological defects,

$$v_{\alpha\beta} = \tilde{v}_{\alpha\beta} + v_{s,\alpha\beta}, \quad (10)$$

where both of the components $\tilde{v}_{\alpha\beta}$ and $v_{s,\alpha\beta}$ obey the expression of velocity fields in Eq. (8). Symmetry defects denoted as Θ can arise due to the compactness of $\theta_{1,2}$, which have the following general solutions:

$$\Theta \equiv (\theta_1, \theta_2) = \ell \left(\frac{y}{a} \varphi(\mathbf{r}) - \frac{x}{a} \ln \frac{r}{a}, -\frac{x}{a} \varphi(\mathbf{r}) - \frac{y}{a} \ln \frac{r}{a} \right). \quad (11)$$

Here a is the size of the defect core and a multi-valued function $\varphi(\mathbf{r})$ is the angle of \mathbf{r} relative to the core. The defect charge ℓ is quantized as a momentum that is well-understood on a lattice. The general rules of constructing symmetry defects have been established in Ref. [22].

III. PHASE-I: DEFECTS ARE CONFINED IN QUADRUPOLES

We consider N defects $\{\Theta_i\}$ carrying winding number (i.e., "charge") ℓ_i with the core coordinates \mathbf{r}_i ($i = 1, \dots, N$), and then the total energy can be expressed in the momentum space:

$$\mathcal{E}[\{\Theta_i\}] = \frac{\rho_0}{2} \sum_{i,j=1}^N \ell_i \ell_j \int d^2\mathbf{q} \mathcal{U}_{\mathbf{q}} e^{i\mathbf{q}\cdot(\mathbf{r}_i - \mathbf{r}_j)}, \quad (12)$$

where $\mathcal{U}_{\mathbf{q}} = \frac{2}{q^4}$ and the momentum $q = |\mathbf{q}|$. In this expression, a series of severely infrared divergent terms can be identified. By observing

$$\int d^2\mathbf{q} \mathcal{U}_{\mathbf{q}} e^{i\mathbf{q}\cdot(\mathbf{r}_i - \mathbf{r}_j)} = 2\pi \left(\frac{L}{a} \right)^2 - \pi \frac{|\mathbf{r}_i - \mathbf{r}_j|^2}{a^2} \ln \frac{L}{a} + f, \quad (13)$$

we can single out two types of divergence, i.e., L^2 and $\ln L$, while the letter f incorporates all finite terms. In the low temperature region, we have to impose the constraints on the defect configuration for energetic consideration. Suppression of

the L^2 divergence requires the net charges vanish, i.e.,

$$\sum_{i=1}^N \ell_i = 0. \quad (14)$$

Under the charge neutral condition, suppression of $\ln L$ divergence further requires the net dipole moments vanish, i.e.,

$$\sum_{i=1}^N \ell_i \mathbf{r}_i = 0. \quad (15)$$

Once both conditions are satisfied, all divergence in Eq. (13) disappears, yielding the screened interacting energy:

$$\mathcal{I}[\Theta_i, \Theta_j] = \pi\rho_0 \sum_{i,j} \ell_i \ell_j \frac{|\mathbf{r}_i - \mathbf{r}_j|^2}{a^2} \ln \frac{|\mathbf{r}_i - \mathbf{r}_j|}{a}. \quad (16)$$

Despite being canceled out, the divergence in Eq. (13) physically allows us to respectively define self-energy formulas of three distinct objects, namely, a single defect, a dipole bound state (BS), and a quadrupole BS:

1. **Divergence of self-energy of a single defect.** The self-energy ($\mathcal{E}_{\text{self}}^s$) of a single defect is polynomially divergent ($\sim L^2$) as $L \rightarrow \infty$:

$$\mathcal{E}_{\text{self}}^s = \pi\rho_0 \ell^2 \left(\frac{L}{a} \right)^2 \rightarrow \infty \quad (17)$$

which is apparently different from the logarithmic divergent self-energy of vortices (i.e., defects) in the conventional KT physics.

2. **Divergence of self-energy of a dipole bound state.** The self-energy ($\mathcal{E}_{\text{self}}^d$) of a dipole BS formed by two defects with opposite charges $\pm\ell$ is logarithmically divergent ($\sim \ln L$) as $L \rightarrow \infty$:

$$\mathcal{E}_{\text{self}}^d = \pi\rho_0 \left(\frac{p}{a} \right)^2 \ln \frac{L}{a} \rightarrow \infty \quad (18)$$

with $p = |\mathbf{p}|$ and $\mathbf{p} = \ell\xi \equiv \ell(\mathbf{r}_1 - \mathbf{r}_2)$ being the dipole moment. Thus, from the expression of self-energy, a dipole BS here resembles a vortex in the conventional KT physics.

3. **Finiteness of self-energy of a quadrupole bound state.** A quadrupole BS is formed by four defects with vanishing charges and vanishing dipole moments, as shown in Fig. 1(a). Its self-energy ($\mathcal{E}_{\text{self}}^q$) is given by ($\Delta_\pm \equiv |\xi \pm \zeta|$, $\xi = |\xi|$, $\zeta = |\zeta|$):

$$\mathcal{E}_{\text{self}}^q = \pi\rho_0 \left(\sum_{\iota=\pm} \frac{\Delta_\iota^2}{a^2} \ln \frac{\Delta_\iota}{a} - 2 \sum_{\tau=\xi,\zeta} \frac{\tau^2}{a^2} \ln \frac{\tau}{a} \right) < \infty. \quad (19)$$

The finiteness of this self-energy is expected since the definition of quadrupole BSs exactly meets the aforementioned two conditions.

Bearing the above analysis in mind, we conclude that, at the thermodynamic limit, HRS defects are energetically confined into quadrupole BSs at low temperatures (Phase-I in Fig. 1). Phase-I shows the algebraic long-range order since the correlation function $\langle \hat{\Phi}(\mathbf{r}_1) \hat{\Phi}^\dagger(\mathbf{r}_2) \rangle$ behaves as a power-law function at long distances due to the gapless phonon mode excitations with a stiffness renormalized by defects.

IV. PHASE-II: DEFECTS ARE CONFINED IN DIPOLES

A. General properties of Phase-II

When the temperature is increased to some critical value T_{c1} , dipole BSs are completely released from quadrupole BSs and proliferate wildly, which leads to a topological phase transition (named as “the first KT transition”) from Phase-I to Phase-II. In Phase-II, the superfluidity is fully destroyed, and thus we do not need to consider the gapless phonon excitations. Instead, the system consists of mobile dipole BSs, while a few defects Θ can be thermally activated. Since a dipole BS is by definition formed by two Θ 's with opposite charges, we can deduce the Hamiltonian of the interacting dipole BSs directly from Eq. (16):

$$H_D = \int d^2\mathbf{q} \sum_{\alpha\beta} \left(\frac{\rho_0 q_\alpha q_\beta}{q^4} + \delta_{\alpha\beta} \mathcal{E}_d \right) D_\alpha(\mathbf{q}) D_\beta(-\mathbf{q}), \quad (20)$$

where $\mathbf{D}(\mathbf{q}) \equiv (D_1(\mathbf{q}), D_2(\mathbf{q}))$ is the dipole BS density field. \mathcal{E}_d is the dipole BS core energy. We leave the concrete derivation of this Hamiltonian to Sec. IV B. Physically, the first term in Eq. (20) accounts for the self-energy divergence shown in Eq. (18) while the second term is the core energy. When temperature increases, dipole BSs reach high density, which will substantially renormalize the interaction (16) between two bare defects Θ .

To analytically understand the phase transition, we introduce the dipole BS fugacity $y_d \equiv \exp(-\beta \mathcal{E}_d)$ where β is the inverse temperature. In general, by definition, a dipole BS is a stable BS object when $\mathcal{E}_d < 2\mathcal{E}_s$ with \mathcal{E}_s being the core energy of a single defect Θ . The thermally activated dipole BSs can weaken the superfluid stiffness ρ , which can be justified via the perturbative RG analysis. It should be noted that, in the RG calculation of the first KT transition, it is enough to keep track of the renormalization effect of released dipole BSs on superfluidity since an isolated defect Θ suffers from much severe energy divergence than a dipole BS. The β -equations for the superfluid stiffness ρ and the fugacity y_d are given by:

$$\frac{d\rho^{-1}}{dl} = 2\beta y_d^2 + \mathcal{O}(y_d^4), \quad (21)$$

$$\frac{dy_d}{dl} = (2 - \pi\beta\rho)y_d + \mathcal{O}(y_d^2), \quad (22)$$

where the dimensionless parameter l parametrizes the RG flows. We leave the detailed derivation of these two β -functions to Sec. IV C. As the right-hand side of Eq. (21) is

positive-definite, we can find the critical temperature

$$T_{c1} = \frac{\pi\rho_0}{2} \quad (23)$$

at the sign change point of the factor “ $(2 - \pi\beta\rho)$ ” in Eq. (22). Alternatively, T_{c1} can be simply obtained by a free energy argument in which sign change of the free-energy of a test object (i.e., an externally inserted dipole BS) occurs at T_{c1} . The derivation in the argument is almost the same as that in the conventional KT physics except that the test object here is not a vortex (defect) but a dipole BS.

B. Hamiltonian formalisms in terms of defect density fields

The defects Θ are the building blocks for dipole and quadrupole BSs. Hence, we can unify the description of defect interaction. Given a defect system, in general, it contains isolated defects Θ , dipole BSs and the quadrupole BSs. For the sake of clarification, we particularly refer to the isolated defects Θ to distinguish ones that are confined in BSs. Nevertheless, a density field $s(\mathbf{r})$ can be defined for the total defects Θ , including both isolated and confined ones, $s(\mathbf{r}) = \sum_i \ell_i \delta(\mathbf{r} - \mathbf{r}_i)$, where ℓ_i is the defect charge and \mathbf{r}_i is the position of the defect core. In this subsection, we will derive a unified Hamiltonian for defect interaction by means of the defect density $s(\mathbf{r})$.

A dipole BS is formed by two neighboring defects Θ with opposite charges $\pm\ell$ that are separated by $\boldsymbol{\xi}$,

$$\ell\Theta(\mathbf{r}) - \ell\Theta(\mathbf{r} - \boldsymbol{\xi}) = \ell\boldsymbol{\xi} \cdot \nabla\Theta(\mathbf{r}). \quad (24)$$

Here we use the notation Θ to denote a defect with charge $\ell = 1$. Accordingly, we introduce the density of dipole BSs

$$\mathbf{D}(\mathbf{r}) \equiv \sum_i \ell_i \left(\frac{\xi_{ix}}{a}, \frac{\xi_{iy}}{a} \right) \delta(\mathbf{r} - \mathbf{r}_i) \equiv \sum_i \mathbf{p}_i \delta(\mathbf{r} - \mathbf{r}_i), \quad (25)$$

while on a lattice, ξ_{ix}/a and ξ_{iy}/a take integer values. Here, \mathbf{p}_i is the dipole moment of the i th dipole BS. From the relation in Eq. (24), we reach a condition $s(\mathbf{r}) = -a\nabla \cdot \mathbf{D}(\mathbf{r})$, where $s(\mathbf{r})$ represents the density of confined defects Θ in a dipole BS.

Similarly, a quadrupole BS consists of four defects Θ ,

$$\begin{aligned} & \ell\Theta(\mathbf{r}) - \ell\Theta(\mathbf{r} - \boldsymbol{\xi}) - \ell\Theta(\mathbf{r} - \boldsymbol{\zeta}) + \ell\Theta(\mathbf{r} - \boldsymbol{\xi} - \boldsymbol{\zeta}) \\ &= \sum_{\alpha,\beta} \ell\xi_\alpha \zeta_\beta \partial_\alpha \partial_\beta \Theta(\mathbf{r}), \end{aligned} \quad (26)$$

where $\alpha, \beta = 1, 2$ and $\partial_\alpha \partial_\beta \Theta(\mathbf{r})$ represents the configuration of a quadrupole BS. Thus, we can introduce a quadrupole BS density, $Q_{\alpha\beta}(\mathbf{r}) = \sum_i \ell_i \frac{\xi_{i\alpha} \zeta_{i\beta}}{a^2} \delta(\mathbf{r} - \mathbf{r}_i)$, which can be related to the density of defect Θ via $s(\mathbf{r}) = a^2 \sum_{\alpha,\beta} \partial_\alpha \partial_\beta Q_{\alpha\beta}(\mathbf{r})$.

In summary, for a defect system, if we apply the notations $\bar{s}(\mathbf{r})$, $\mathbf{D}(\mathbf{r})$ and Q respectively for isolated defect density, density of dipole BSs and density of quadrupole BSs, along with $s(\mathbf{r})$ as the density of all defects Θ , we have the condition,

$$s(\mathbf{r}) = \bar{s}(\mathbf{r}) - a\nabla \cdot \mathbf{D}(\mathbf{r}) + a^2 \sum_{\alpha,\beta} \partial_\alpha \partial_\beta Q_{\alpha\beta}(\mathbf{r}). \quad (27)$$

With the concrete configuration of defects Θ in Eq. (11), the corresponding velocity field $v_{s,\alpha\beta}(\mathbf{r})$ can be evaluated as

$$\begin{aligned} v_{s,\alpha\beta}(\mathbf{r}) &= - \sum_i \ell_i \delta_{\alpha\beta} \left(-1 - \ln \frac{|\mathbf{r} - \mathbf{r}_i|}{a} \right) \\ &= - \int d^2 \mathbf{r}' \delta_{\alpha\beta} \left(-1 - \ln \frac{|\mathbf{r} - \mathbf{r}'|}{a} \right) s(\mathbf{r}') \\ &= \int d^2 \mathbf{q} \delta_{\alpha\beta} \frac{s(\mathbf{q})}{q^2} e^{i\mathbf{q}\cdot\mathbf{r}} \end{aligned} \quad (28)$$

which simply indicates a relation between velocity fields $v_{s,\alpha\beta}$ and the defect density $s(\mathbf{q})$: $v_{s,\alpha\beta}(\mathbf{q}) = \delta_{\alpha\beta} \frac{s(\mathbf{q})}{q^2}$. Therefore, we can alternatively characterize the defect system by a unified Hamiltonian,

$$H = \frac{\rho_0}{2} \int d^2 \mathbf{q} \frac{2}{q^4} s(\mathbf{q}) s(-\mathbf{q}), \quad (29)$$

where $s(\mathbf{q})$ is a density of total defects Θ . From Eq. (29), one can also recover the defect interaction. For example, when $s(\mathbf{r}) = -a \nabla \cdot \mathbf{D}(\mathbf{r})$, we have the Hamiltonian (20) for interacting dipole BSs by adding the core energy term.

C. Renormalization group analysis of the first KT transition

To describe how the topological defects reduce the superfluid stiffness, we have to integrate out the topological defects, which is represented in terms of velocity field $v_{s,\alpha\beta}$. The resulting free energy is

$$F(\tilde{v}_{\alpha\beta}) = -T \ln \int Dv_{s,\alpha\beta} \exp(-\beta H), \quad (30)$$

where

$$H = \frac{\rho_0}{2} \int d^2 \mathbf{r} \sum_{\alpha\beta} (\tilde{v}_{\alpha\beta}^2 + 2\tilde{v}_{\alpha\beta} v_{s,\alpha\beta} + v_{s,\alpha\beta}^2), \quad (31)$$

and $\tilde{v}_{\alpha\beta}$ is the velocity field in the absence of defects. The renormalization effect can be measured by the change of a free energy in response to a small constant velocity shift to the smooth component $\tilde{v}_{\alpha\beta} \rightarrow \tilde{v}_{\alpha\beta} + u_{\alpha\beta}$,

$$F(\tilde{v}_{\alpha\beta} + u_{\alpha\beta}) - F(\tilde{v}_{\alpha\beta}) = \frac{1}{2} \Omega \rho_R \sum_{\alpha\beta} u_{\alpha\beta}^2 + \mathcal{O}(u_{\alpha\beta}^4), \quad (32)$$

where ρ_R is the renormalized superfluid stiffness

$$\rho_R = \frac{1}{\Omega} \frac{\delta^2 F(\tilde{v}_{\alpha\beta} + u_{\alpha\beta})}{\delta u_{\alpha\beta} \delta u_{\alpha\beta}} \Big|_{u=0}, \quad (33)$$

and Ω is the system area. In the dilute limit, after averaging over defect configuration, we can extract ρ_R ,

$$\begin{aligned} \rho_R &= \rho_0 - \beta \rho_0^2 \int d^2 \mathbf{r} \sum_{\alpha\beta} \langle v_{s,\alpha\beta}(\mathbf{r}) v_{s,\alpha\beta}(0) \rangle \\ &= \rho_0 - \beta \rho_0^2 \lim_{q \rightarrow 0} \frac{2}{q^4} \langle s(\mathbf{q}) s(-\mathbf{q}) \rangle, \end{aligned} \quad (34)$$

where $\langle \cdot \rangle$ averages over all defect configurations and the relation “ $v_{s,\alpha\beta}(\mathbf{q}) = \delta_{\alpha\beta} \frac{s(\mathbf{q})}{q^2}$ ” is adopted. The formula in Eq. (34) is our starting point to derive the RG equation of KT transition. The remaining task is to compute the correlator $\langle s(\mathbf{q}) s(-\mathbf{q}) \rangle$.

Topological defects Θ are confined into quadrupoles in the low temperature. As the temperature increases, the quadrupole BSs begin to disassociate into dipole BSs at the first transition and then dipole BSs fully split into freely movable defects Θ at the second transition. Physically, the creation of an isolated defect or a dipole BS requires positive chemical potential, thus, we consider the core energy \mathcal{E}_s for an isolated defect and the core energy \mathcal{E}_d for a dipole BS. As the formation of the dipole BS will lower the energy, we have to require $\mathcal{E}_d < 2\mathcal{E}_s$ in general.

Around the first transition, dipole BSs can be thermally activated to reduce the superfluid stiffness. Thus, a system with only dipole BSs is considered here and we need to evaluate the dipole BS contribution to the correlators. In the grand ensemble $\Xi = \sum_{\{\mathbf{D}(\mathbf{r})\}} e^{-\beta H_D}$ and Hamiltonian H_D is given in Eq. (20). In real space,

$$\begin{aligned} H_D &= \frac{1}{2} \rho_0 \int_{|\mathbf{r}-\mathbf{r}'|>a} d^2 \mathbf{r} d^2 \mathbf{r}' \sum_{\alpha\beta} D_\alpha(\mathbf{r}) D_\beta(\mathbf{r}') \\ &\quad \cdot \left(-2\pi \delta_{\alpha\beta} \log \frac{|\mathbf{r} - \mathbf{r}'|}{a} - 2\pi \frac{(r_\alpha - r_\beta)(r'_\alpha - r'_\beta)}{|\mathbf{r} - \mathbf{r}'|^2} \right) \\ &\quad + \mathcal{E}_d \int d^2 \mathbf{r} \mathbf{D}^2(\mathbf{r}). \end{aligned} \quad (35)$$

The system should meet the dipole charge neutral condition $\sum_i \mathbf{p}_i = 0$. In the low energy limit, since the core energy is large as compared with the temperature, and the dipole BSs are dilute, we can calculate physical quantity in a power series of the fugacity $y_d = e^{-\beta \mathcal{E}_d}$. With the dipole charge neutral condition and the relation between $s(\mathbf{q})$ and $\mathbf{D}(\mathbf{q})$, we can express the defect correlator in terms of dipole BS correlators,

$$\lim_{q \rightarrow 0} \frac{\langle s(\mathbf{q}) s(-\mathbf{q}) \rangle}{q^4} = -\frac{\pi}{2} \sum_{i \neq j} \int_{r_{ij} > a} \frac{dr_{ij}}{a^2} \langle \mathbf{p}_i \cdot \mathbf{p}_j r_{ij}^3 \rangle, \quad (36)$$

where $\mathbf{r}_{ij} = \mathbf{r}_i - \mathbf{r}_j$. In the dilute limit, we can just consider a pair of dipole BSs. Regarding the energy in Eq. (35), there are five cases in the leading order, $\mathbf{p}_i = (1, 0), \mathbf{p}_j = (-1, 0)$ or $\mathbf{p}_i = (-1, 0), \mathbf{p}_j = (1, 0)$ or $\mathbf{p}_i = (0, 1), \mathbf{p}_j = (0, -1)$ or $\mathbf{p}_i = (0, -1), \mathbf{p}_j = (0, 1)$ or $\mathbf{p}_i = \mathbf{p}_j = (0, 0)$. With a fixed separation \mathbf{r}_{ij} , the first four cases have equal contributions to grand ensemble. We hence obtain $\langle \mathbf{p}_i \cdot \mathbf{p}_j r_{ij}^3 \rangle = -4y_d^2 \left(\frac{r_{ij}}{a}\right)^{3-2\pi\beta\rho_0}$, which yields

$$\lim_{q \rightarrow 0} \frac{\langle s(\mathbf{q}) s(-\mathbf{q}) \rangle}{q^4} = 2\pi y_d^2 \int_{r>a} \frac{dr}{a} \left(\frac{r}{a}\right)^{3-2\pi\beta\rho_0} + \mathcal{O}(y_d^4). \quad (37)$$

We are ready to send Eq. (37) back to Eq. (34). After keeping the lowest order in ρ_R^{-1} , we have

$$\rho_R^{-1} = \rho_0^{-1} - 2\pi \int_{r>a} \frac{dr}{a} \left(\frac{r}{a}\right)^{3-2\pi\beta\rho_0} + \mathcal{O}(y_d^4). \quad (38)$$

The RG equation arises when we enforce the standard regularization scheme by dividing the integral into two parts, $\int_{r>a} = \int_a^{ae^{\delta l}} + \int_{ae^{\delta l}}^\infty$ which leads to two equations,

$$\rho_R^{-1} = \rho^{-1}(\delta l) + 2\pi\beta y_d^2 \int_{ae^{\delta l}}^{+\infty} \frac{d\xi}{a} \left(\frac{\xi}{a}\right)^{3-2\pi\beta\rho_0} + \mathcal{O}(y_d^4) \quad (39)$$

and

$$\rho^{-1}(\delta l) = \rho_0^{-1} + 2\pi\beta y_d^2 \int_a^{ae^{\delta l}} \frac{d\xi}{a} \left(\frac{\xi}{a}\right)^{3-2\pi\beta\rho_0} + \mathcal{O}(y_d^4). \quad (40)$$

Substituting Eq. (40) into Eq. (39) yields the renormalized fugacity, $y(\delta l) = ye^{(2-\beta\rho_0)\delta l}$. Therefore, we reach the RG equations (21) and (22) for the first transition at T_{c1} . Above T_{c1} , the superfluid stiffness gets renormalized into $\rho_R \rightarrow 0$, indicating that the superfluid phase is broken down. We then goes to a phase with the dipole BSs as freely mobile charge carriers. In deriving the RG equations, we have introduced a lattice regularization on which the dipole charges can only take integer values. Also, one can repeat the above procedures in a continuum space, in which $\mathbf{p}_i \cdot \mathbf{p}_j = \ell_i \ell_j \boldsymbol{\xi}_i \cdot \boldsymbol{\xi}_j$ includes a part from the relative angular $\boldsymbol{\xi}_i \cdot \boldsymbol{\xi}_j = \xi_i \xi_j \cos(\theta_{ij})$. It will alter the coefficient before y^2 , but the physics will not be changed.

V. PHASE-III: DEFECTS ARE DECONFINED

A. General properties of Phase-III

When the temperature is close to the topological phase transition (named as ‘‘the second KT transition’’) from Phase-II to Phase-III, dipole BSs form a plasma due to sufficiently high density and equivalently we have a condensate of dipole BSs. Therefore, the interaction between two defects Θ , i.e., \mathcal{I} in Eq. (16) gets strongly screened. This dynamical renormalization can be quantitatively treated via the standard Debye-Hückel approximation by approximating the dipole BSs as a continuous independent field. At low energies and small \mathbf{q} , we keep the leading orders, yielding an effective Hamiltonian for defects:

$$H_{\text{eff}} = \int d^2\mathbf{q} \left[\frac{\mathcal{E}_d}{q^2} + (\mathcal{E}_s - \rho_0\lambda_d^4) \right] s(\mathbf{q})s(-\mathbf{q}), \quad (41)$$

where $s(\mathbf{q})$ is the Fourier transformation of a defect density $s(\mathbf{r}) \equiv \sum_i \ell_i \delta(\mathbf{r} - \mathbf{r}_i)$ and $\lambda_d = \sqrt{\mathcal{E}_d/\rho_0}$ denotes the Debye-Hückel screening length. The detailed derivation of this Hamiltonian is shown in Sec. VB. Physically, the dipole BS plasma brings two significant effects: 1) to renormalize the interaction from Eq. (16) to $\ln \frac{|\mathbf{r}_i - \mathbf{r}_j|}{a}$; 2) to reduce the core energy to $\mathcal{E}_s - \rho_0\lambda_d^4$. Based on H_{eff} , we can obtain the phase diagram in Fig. 1 via the following analysis of three aspects:

1. When the effective core energy $\mathcal{E}_s - \rho_0\lambda_d^4 > 0$ along with $T_{c2} > T_{c1}$ gives $(2\mathcal{E}_d)^{-1} < \rho_0^{-1} < \mathcal{E}_s/\mathcal{E}_d^2$, i.e., the

domain (A, B) in Fig. 1, the system in Eq. (41) reduces to a 2D Coulomb gas, which has a KT transition at

$$T_{c2} = \pi\mathcal{E}_d. \quad (42)$$

The second KT transition T_{c2} merely depends on the core energy of dipole BSs, which corresponds to the horizontal line separating Phase II and III in Fig. 1.

2. Instability occurs in case of a negative reduced core energy $\mathcal{E}_s - \rho_0\lambda_d^4 < 0$ (i.e., $\rho_0^{-1} > \mathcal{E}_s/\mathcal{E}_d^2$) or $T_{c2} < T_{c1}$ (i.e., $\rho_0^{-1} < (2\mathcal{E}_d)^{-1}$). In the former case, instead, the screening effect favors a finite density of defects Θ , $\langle s(\mathbf{q}) \rangle \neq 0$, when higher-order term is involved in Eq. (41), with a vertical line as a boundary between Phase II and Phase III. In the latter case, Phase II is metastable and the two transitions merge together. In both cases, the intermediate Phase-II between Phase-I and Phase-II does not exist and we end up with a direct transition from Phase-I to Phase-III, where quadrupole BSs are directly dissolved into free defects.
3. At the high temperature limit in Phase-III where defects Θ reach a sufficiently high density, a plasma phase of isolated defects forms. The effective interaction of defects in this phase will be renormalized by the susceptibility $\chi_{ss}(\mathbf{q})$ induced by defect plasma. The effective interaction is

$$\frac{2\rho_0}{q^4} - \rho_0\chi_{ss}(\mathbf{q}) = \frac{2\rho_0}{q^4 + \lambda_s^{-4}}, \quad (43)$$

where λ_s is the temperature-dependent Debye-Hückel screening length of defects Θ and we can find that the screening effect leads to a short ranged interaction. Thus, in Phase-III, defects are called Calypso in Introduction. We leave the concrete derivation of the effective interaction in Sec. VC.

B. Debye-Hückel approximation and the second KT transition

Around the second transition point, the density of quadrupole BSs vanishes, $Q_{\alpha\beta} = 0$. At the stage, the Hamiltonian only involves isolated defect density $\bar{s}(\mathbf{r})$ and dipole BS density $\mathbf{D}(\mathbf{r})$,

$$H = \frac{\rho_0}{2} \int d^2q \frac{2}{q^4} s(\mathbf{q})s(-\mathbf{q}) + \int d^2r [\mathcal{E}_s \bar{s}^2(\mathbf{r}) + \mathcal{E}_d \mathbf{D}^2(\mathbf{r})], \quad (44)$$

where the total defect density $s(\mathbf{r}) = \bar{s}(\mathbf{r}) - \nabla \cdot \mathbf{D}(\mathbf{r})$. The dipole BSs have sufficiently high density to form a plasma, which allows us to apply the Debye-Hückel approximation and to take the density $\mathbf{D}(\mathbf{r})$ as a continuous function. The first terms in Eq. (44) contains the coupling terms between isolated defects $\bar{s}(\mathbf{q})$ and dipole BSs $\mathbf{D}(\mathbf{q})$, i.e.

$$\begin{aligned} \frac{1}{q^4} s(\mathbf{q})s(-\mathbf{q}) &= \frac{1}{q^4} \bar{s}(\mathbf{q})\bar{s}(-\mathbf{q}) + 2 \sum_{\alpha} \frac{i q_{\alpha}}{q^4} \bar{s}(\mathbf{q}) D_{\alpha}(-\mathbf{q}) \\ &+ \sum_{\alpha\beta} \frac{q_{\alpha} q_{\beta}}{q^4} D_{\alpha}(\mathbf{q}) D_{\beta}(-\mathbf{q}). \end{aligned} \quad (45)$$

The plasma of dipole BSs can screen the interaction between defects. We first evaluate the correlator of dipole bound state. Notice that the partition function for the dipole BSs is $\Xi_d = \int \mathcal{D}\mathbf{D} \exp(-\beta H_d)$, where

$$H_d = \int d^2q \sum_{\alpha\beta} \left(\rho_0 \frac{q_\alpha q_\beta}{q^4} + \delta_{\alpha\beta} \mathcal{E}_d \right) D_\alpha(\mathbf{q}) D_\beta(-\mathbf{q}) \quad (46)$$

Here, $\mathbf{D}(\mathbf{q})$ is a continuous function by taking the Debye-Hückle approximation. Thus, the correlator can be calculated by Gaussian integral,

$$\begin{aligned} & \langle D_\alpha(\mathbf{q}) D_\beta(-\mathbf{q}) \rangle \\ &= \frac{1}{\mathcal{E}_d} \left[\left(\delta_{\alpha\beta} - \frac{q_\alpha q_\beta}{q^2} \right) + \frac{q_\alpha q_\beta}{q^2} \frac{q^2}{\lambda_d^{-2} + q^2} \right], \quad (47) \end{aligned}$$

where $\lambda_d = \sqrt{\mathcal{E}_d/\rho_0}$ is the Debye-Hückel screening length of dipole BSs.

The effective interaction in the dipole BS plasma is renormalized by correlator in Eq. (47),

$$\frac{\rho_0}{q^4} - \sum_{\alpha\beta} \frac{\rho_0^2 q_\alpha q_\beta}{q^8} \langle D_\alpha(\mathbf{q}) D_\beta(-\mathbf{q}) \rangle = \frac{\rho_0}{q^2} \frac{1}{\lambda_d^{-2} + q^2} \quad (48)$$

where the factor $q_\alpha q_\beta/q^8$ is from the coupling term in Eq. (45). With the core energy \mathcal{E}_s for isolated defects, the Hamiltonian for defects in dipole BS plasma is

$$H = \int d^2q \left(\frac{\rho_0}{q^2} \frac{1}{\lambda_d^{-2} + q^2} + \mathcal{E}_s \right) \bar{s}(\mathbf{q}) \bar{s}(-\mathbf{q}) \quad (49)$$

Making the expansion in the low energy will result in the effective Hamiltonian in Eq. (41).

C. The defect plasma and the effective interaction

At high temperature $T \gg T_{c2}$ region, both dipole and quadrupole BSs disassociate into free isolated defects. This is a plasma phase of defects, and then the interactions between defects will get screened. In this case, the Hamiltonian just involves density of isolated defects, which reads

$$H = \frac{\rho_0}{2} \int d^2\mathbf{q} \frac{2}{q^4} s(\mathbf{q}) s(-\mathbf{q}) + \mathcal{E}_s \int d^2\mathbf{r} s^2(\mathbf{r}). \quad (50)$$

We regularize the system with the constant by a lattice with a lattice constant a . Then a plasma phase is referred to as one defect per site, $\sum_{\ell \neq 0} n_\ell(\mathbf{r}) = 1$, where $n_\ell(\mathbf{r})$ is the number of a defect with charge ℓ at site \mathbf{r} , $n_\ell(\mathbf{r}) = \sum_i \delta_{\ell, \ell_i} \delta(\mathbf{r} - \mathbf{r}_i)$ with a relation $\bar{s}(\mathbf{r}) = \sum_\ell \ell n_\ell(\mathbf{r})$. Then, we reformulate the Hamiltonian in (50)

$$\begin{aligned} H &= \frac{\rho_0}{2} \int d^2\mathbf{r} d^2\mathbf{r}' \sum_{\ell, \ell'} \ell \ell' n_\ell(\mathbf{r}) U(\mathbf{r} - \mathbf{r}') n_{\ell'}(\mathbf{r}') \\ &+ \mathcal{E}_s \int d^2\mathbf{r} \sum_\ell \ell^2 n_\ell(\mathbf{r}), \quad (51) \end{aligned}$$

where $U(\mathbf{r})$ is the Fourier transformation of $2/q^4$. $n_\ell(\mathbf{r})$ is a function of the position \mathbf{r}_i of the individual defects. In order to obtain the interaction screened by the plasma, we decompose all the defects $n_\ell(\mathbf{r})$ into the continuous plasma field $\langle n_\ell(\mathbf{r}) \rangle$ and the additional defects placed in the plasma $\delta n_\ell(\mathbf{r})$, $n_\ell(\mathbf{r}) = \langle n_\ell(\mathbf{r}) \rangle + \delta n_\ell(\mathbf{r})$. Keeping the terms containing $\langle n_\ell(\mathbf{r}) \rangle$, we have the free energy at the mean-field level [3]

$$\begin{aligned} F &= \frac{\rho_0}{2} \int d^2\mathbf{r} d^2\mathbf{r}' \sum_{\ell, \ell'} \ell \ell' \langle n_\ell(\mathbf{r}) \rangle U(\mathbf{r} - \mathbf{r}') \langle n_{\ell'}(\mathbf{r}') \rangle - \int d^2\mathbf{r} \sum_\ell \ell \langle n_\ell(\mathbf{r}) \rangle \phi^{\text{ext}}(\mathbf{r}) \\ &+ \mathcal{E}_s \int d^2\mathbf{r} \sum_\ell \ell^2 \langle n_\ell(\mathbf{r}) \rangle + \frac{1}{\beta} \sum_\ell \int d^2\mathbf{r} \langle n_\ell(\mathbf{r}) \rangle \ln \langle n_\ell(\mathbf{r}) \rangle, \quad (52) \end{aligned}$$

with an external field $\phi^{\text{ext}}(\mathbf{r}) = \sum_\ell \ell \delta n_\ell(\mathbf{r}) U(\mathbf{r} - \mathbf{r}')$. In the equilibrium, minimize F under the condition $\sum_{\ell \neq 0} n_\ell(\mathbf{r}) = 1$ and we obtain the mean field solution

$$\langle n_\ell(\mathbf{r}) \rangle = \frac{\exp \left[\beta \ell \phi^{\text{ext}}(\mathbf{r}) - \beta \ell^2 \mathcal{E}_s - \beta \ell \rho_0 \int d^2\mathbf{r}' \sum_{\ell' \neq 0} \ell' \langle n_{\ell'}(\mathbf{r}') \rangle U(\mathbf{r} - \mathbf{r}') \right]}{\sum_{\ell \neq 0} \exp \left[\beta \ell \phi^{\text{ext}}(\mathbf{r}) - \beta \ell^2 \mathcal{E}_s - \beta \ell \rho_0 \int d^2\mathbf{r}' \sum_{\ell' \neq 0} \ell' \langle n_{\ell'}(\mathbf{r}') \rangle U(\mathbf{r} - \mathbf{r}') \right]}. \quad (53)$$

The effective interaction for $\delta n_\ell(\mathbf{r})$ can be yielded by the linear response function

$$\chi_{ss}(\mathbf{r}, \mathbf{r}') = \sum_\ell \ell \left. \frac{\delta \langle n_\ell(\mathbf{r}) \rangle}{\delta \phi^{\text{ext}}(\mathbf{r}')} \right|_{\phi^{\text{ext}}=0}. \quad (54)$$

In response to fluctuation field $\phi^{\text{ext}}(\mathbf{r})$, the $\langle n_\ell(\mathbf{r}) \rangle$ is changed according to Eq. (53). We can evaluate the suscepti-

bility $\chi_{ss}(\mathbf{r}, \mathbf{r}')$ as

$$\chi_{ss}(\mathbf{r}, \mathbf{r}') = \frac{\rho_0 \mathcal{E}_s}{2\lambda_s^4 \mathcal{E}_c} \left[\delta(\mathbf{r} - \mathbf{r}') - \rho_0 \int d^2 \mathbf{r}'' \chi_{ss}(\mathbf{r}'', \mathbf{r}') U(\mathbf{r} - \mathbf{r}'') \right], \quad (55)$$

and in the momentum space,

$$\chi_{ss}(\mathbf{q}) = \left(\frac{2\rho_0}{q^4} + \frac{2\rho_0 \lambda_s^4 \mathcal{E}_c}{\mathcal{E}_s} \right)^{-1}, \quad (56)$$

with a coefficient $\lambda_s = \left(\frac{2\rho_0 \sum_{\ell \neq 0} \beta \mathcal{E}_c \ell^2 e^{-\beta \mathcal{E}_s \ell^2}}{\mathcal{E}_s \sum_{\ell \neq 0} e^{-\beta \mathcal{E}_s \ell^2}} \right)^{-1/4}$. In the high temperature limit, we have $\beta \mathcal{E}_s \rightarrow 0$ and $\lambda_s = (\rho_0 / \mathcal{E}_s)^{-1/4}$. With susceptibility $\chi_{ss}(\mathbf{q})$ describing the screening effect, the interaction of defects reduces to a short ranged interaction in Eq. (43).

VI. GENERALIZATION

The above discussion can be generalized to defects of a general higher-rank symmetry group with multi-moment conservation. As a result, a minimal bound state formed by defects carrying opposite topological charges to reach neutralization, resembles a local particle with a finite energy. Consider a system containing N defects at $\mathbf{r}_i, i = 1, \dots, N$ with topological charges $\ell_i, i = 1, \dots, N$. The total energy can be formulated as

$$\mathcal{E} = \sum_{i,j} \ell_i \ell_j \int d^2 \mathbf{q} \mathcal{U}_{\mathbf{q}} e^{i\mathbf{q} \cdot (\mathbf{r}_i - \mathbf{r}_j)}, \quad (57)$$

where $\mathcal{U}_{\mathbf{q}}$ describes defect interaction and generally we assume $\mathcal{U}_{\mathbf{q}} \propto 1/q^{2n}$ ($n \in \mathbb{Z}$) at low energies, i.e., the IR limit with small momentum q , which leads to energy divergence of a single defect. We can expose the divergent features:

$$\int d^2 \mathbf{q} \mathcal{U}_{\mathbf{q}} e^{i\mathbf{q} \cdot (\mathbf{r}_i - \mathbf{r}_j)} \propto \int d^2 \mathbf{q} \frac{P_{2n-2}}{q^{2n}} + \text{finite} \quad (58)$$

with $P_n(\mathbf{r}) = \sum_{k=0}^n \frac{(i\mathbf{q} \cdot \mathbf{r})^k}{k!}$ and finite denoting the remaining non-divergent terms. By inspecting the power-law and logarithmic divergence, we have the BS that can be thermally activated from the ground states with conservation of the first m -th moments

$$Q_{\alpha_1 \alpha_2 \dots \alpha_n} \equiv \sum_i \ell_i r_{i\alpha_1} r_{i\alpha_2} \dots r_{i\alpha_n} = 0, n \leq m. \quad (59)$$

We fix our attention on defects carrying topological charges ± 1 , and at low energies, the minimal BS with the first $2n$ th moments vanishing, contain 2^n defects, with half $\ell = +1$ and half $\ell = -1$ and the spatial alignment of these vortices is strongly constrained.

Accordingly, we can establish a series of KT topological transitions that successively occur at different temperatures due to proliferation of defects and defect BSs. The effect

of hierarchical proliferation can be theoretically characterized by means of RG flow equations and the Debye-Hückel approximation. More interestingly, a screening effect from sufficiently high density of defect BSs can lead to instability and collapse of the intermediate temperature phases, which further enriches the phase diagrams. In particular, the first KT point is determined by the stiffness, while the other ones are related to the BS core energies.

VII. SUMMARY AND OUTLOOK

As an important ingredient of the series of works on fractonic superfluids, in this paper, we have systematically investigated the finite-temperature phase structure of fractonic superfluids, where the conventional $\mathbb{U}(1)$ symmetry is replaced by higher rank symmetry and the conventional superfluid vortex is replaced by higher rank symmetry defect. A hierarchical proliferation of topological objects has been identified, resulting in a finite-temperature phase diagram shown in Fig. 1. The model in Eq. (1) can be promisingly realizable in the cold atomic gas subjected to an optical lattice by tuning a two-particle state [28]. Eq. (42) indicates that T_{c2} is determined by \mathcal{E}_d , i.e., the core energy of dipole-like BSs of defects. Naively, a core energy manifests as the increase in free energy due to destruction of the superfluidity, i.e., $\mathcal{E}_d \sim a^2 f_{\text{cond}}$ with f_{cond} being the superfluid energy density. Along with the Josephson scaling relation $\rho(T) \sim T_c \xi$ and $f_{\text{cond}} \sim T_c \xi^{-2}$, we can estimate the core energy $\mathcal{E}_d \sim \pi \rho_0 / 2$ at the optimal value of a that minimizes the total energy $\mathcal{E}_{\text{self}}^d + \mathcal{E}_d$ of a single dipole BS with a unit charge. Simultaneously, a numerical simulation on a proper lattice regularized model is desired to benchmark the phase diagram in Fig. 1 by incorporating the defect core physics. One may also decorate these defects [29] and then defect condensation [30–33] may generate new classes of Symmetry Protected Topological (SPT) phases beyond group cohomology [34]. The non-equilibrium properties are also of fundamental importance, since the high rank symmetry enforces dynamics with constraint kinetics. Example is the Kibble-Zurek mechanism of the forming of high-rank defects that is triggered through a continuous phase transition at finite rate. Recently, HRS has attracted much attention from fields other than condensed matter physics, see, e.g., Refs. [27, 35–38]. It is interesting to study effect of defects. The corresponding response theory may involve exotic geometric (gravitational) response, leading to, potentially, exotic topological terms, e.g., mixture of Riemann-Cartan quantities and fibre bundle of internal gauge fields, and twisted topological terms [30, 31, 39–45].

ACKNOWLEDGMENTS

The first two authors (J.K.Y. and S.A.C.) contributed equally to this work. The authors acknowledge helpful discussions with T.K. Ng, K.T. Law and Y.B. Yang. This work was supported by Guangdong Basic and Applied Basic Research Foundation under Grant No. 2020B1515120100, NSFC Grant

(No. 12074438). The work reported here was performed on resources provided in part by the Guangdong Provincial Key

Laboratory of Magnetoelectric Physics and Devices (LaM-Pad).

-
- [1] J. M. Kosterlitz and D. J. Thouless, *Journal of Physics C: Solid State Physics* **6**, 1181 (1973).
- [2] J. M. Kosterlitz, *Reports on Progress in Physics* **79**, 026001 (2016).
- [3] P. M. Chaikin and T. C. Lubensky, *Principles of condensed matter physics*, Vol. 1 (Cambridge university press Cambridge, 2000).
- [4] R. M. Nandkishore and M. Hermele, *Annual Review of Condensed Matter Physics* **10**, 295 (2019), arXiv:1803.11196 [cond-mat.str-el].
- [5] M. Pretko, X. Chen, and Y. You, *International Journal of Modern Physics A* **35**, 2030003 (2020), arXiv:2001.01722 [cond-mat.str-el].
- [6] C. Chamon, *Phys. Rev. Lett.* **94**, 040402 (2005).
- [7] J. Haah, *Phys. Rev. A* **83**, 042330 (2011).
- [8] S. Vijay, J. Haah, and L. Fu, *Phys. Rev. B* **92**, 235136 (2015).
- [9] S. Vijay, J. Haah, and L. Fu, *Phys. Rev. B* **94**, 235157 (2016).
- [10] M. Pretko, *Phys. Rev. B* **95**, 115139 (2017).
- [11] H. Ma, E. Lake, X. Chen, and M. Hermele, *Phys. Rev. B* **95**, 245126 (2017).
- [12] D. J. Williamson and T. Devakul, *Phys. Rev. B* **103**, 155140 (2021).
- [13] S. Moudgalya, A. Prem, R. Nandkishore, N. Regnault, and B. A. Bernevig, arXiv e-prints, arXiv:1910.14048 (2019), arXiv:1910.14048 [cond-mat.str-el].
- [14] W. Shirley, K. Slagle, Z. Wang, and X. Chen, *Phys. Rev. X* **8**, 031051 (2018).
- [15] A. Dua, P. Sarkar, D. J. Williamson, and M. Cheng, *Phys. Rev. Research* **2**, 033021 (2020).
- [16] M.-Y. Li and P. Ye, *Phys. Rev. B* **101**, 245134 (2020).
- [17] M.-Y. Li and P. Ye, *Phys. Rev. B* **104**, 235127 (2021).
- [18] C. Zhou, M.-Y. Li, Z. Yan, P. Ye, and Z. Y. Meng, *Phys. Rev. Research* **4**, 033111 (2022).
- [19] C. Zhou, M.-Y. Li, Z. Yan, P. Ye, and Z. Y. Meng, (2022), arXiv:2209.12917 [cond-mat.str-el].
- [20] M.-Y. Li and P. Ye, (2022), arXiv:2211.14136 [quant-ph].
- [21] J.-K. Yuan, S. A. Chen, and P. Ye, *Physical Review Research* **2**, 023267 (2020), arXiv:1911.02876 [cond-mat.str-el].
- [22] S. A. Chen, J.-K. Yuan, and P. Ye, *Phys. Rev. Research* **3**, 013226 (2021), arXiv:2010.03261 [cond-mat.str-el].
- [23] H. Li and P. Ye, *Physical Review Research* **3**, 043176 (2021), arXiv:2104.03237 [cond-mat.quant-gas].
- [24] J.-K. Yuan, S. A. Chen, and P. Ye, *Chinese Physics Letters* **39**, 057101 (2022).
- [25] C. Stahl, E. Lake, and R. Nandkishore, *Phys. Rev. B* **105**, 155107 (2022), arXiv:2111.08041 [cond-mat.stat-mech].
- [26] A. Kapustin and L. Spodyneiko, arXiv e-prints, arXiv:2208.09056 (2022), arXiv:2208.09056 [cond-mat.str-el].
- [27] R. Argurio, C. Hoyos, D. Musso, and D. Naegels, *Phys. Rev. D* **104**, 105001 (2021).
- [28] H. P. Büchler, M. Hermele, S. D. Huber, M. P. Fisher, and P. Zoller, *Phys. Rev. Lett.* **95**, 040402 (2005), arXiv:cond-mat/0503254 [cond-mat.str-el].
- [29] X. Chen, Y.-M. Lu, and A. Vishwanath, *Nature Communications* **5**, 3507 (2014), arXiv:1303.4301 [cond-mat.str-el].
- [30] A. P. O. Chan, P. Ye, and S. Ryu, *Phys. Rev. Lett.* **121**, 061601 (2018).
- [31] Z.-C. Gu, J. C. Wang, and X.-G. Wen, *Phys. Rev. B* **93**, 115136 (2016).
- [32] P. Ye and Z.-C. Gu, *Phys. Rev. X* **5**, 021029 (2015).
- [33] P. Ye and Z.-C. Gu, *Phys. Rev. B* **93**, 205157 (2016).
- [34] X. Chen, Z.-C. Gu, Z.-X. Liu, and X.-G. Wen, *Science* **338**, 1604 (2012).
- [35] L. Bidussi, J. Hartong, E. Have, J. Musaeus, and S. Prohazka, (2021), arXiv:2111.03668 [hep-th].
- [36] A. Jain and K. Jensen, (2021), arXiv:2111.03973 [hep-th].
- [37] S. Angus, M. Kim, and J.-H. Park, (2021), arXiv:2111.07947 [hep-th].
- [38] K. T. Grosvenor, C. Hoyos, F. Peña Benitez, and P. Surówka, (2021), arXiv:2112.00531 [hep-th].
- [39] B. Han, H. Wang, and P. Ye, *Phys. Rev. B* **99**, 205120 (2019).
- [40] P. Ye and J. Wang, *Phys. Rev. B* **88**, 235109 (2013).
- [41] Z.-F. Zhang and P. Ye, *Phys. Rev. Research* **3**, 023132 (2021).
- [42] M. Cheng and Z.-C. Gu, *Phys. Rev. Lett.* **112**, 141602 (2014).
- [43] P. Ye, M. Cheng, and E. Fradkin, *Phys. Rev. B* **96**, 085125 (2017).
- [44] P. Putrov, J. Wang, and S.-T. Yau, *Annals of Physics* **384**, 254 (2017).
- [45] Z.-F. Zhang, Q.-R. Wang, and P. Ye, (2022), arXiv:2208.09228 [cond-mat.str-el].